

1-1-2013

Planar waveguide with left-handed material guiding film for refractometry applications

TAHER M. EL-AGEZ

SOFYAN A. TAYA

MOHAMED M. SHABAT

HANI M. KULLAB

Follow this and additional works at: <https://journals.tubitak.gov.tr/physics>



Part of the [Physics Commons](#)

Recommended Citation

EL-AGEZ, TAHER M.; TAYA, SOFYAN A.; SHABAT, MOHAMED M.; and KULLAB, HANI M. (2013) "Planar waveguide with left-handed material guiding film for refractometry applications," *Turkish Journal of Physics*: Vol. 37: No. 2, Article 13. <https://doi.org/10.3906/fiz-1206-9>
Available at: <https://journals.tubitak.gov.tr/physics/vol37/iss2/13>

This Article is brought to you for free and open access by TÜBİTAK Academic Journals. It has been accepted for inclusion in Turkish Journal of Physics by an authorized editor of TÜBİTAK Academic Journals. For more information, please contact academic.publications@tubitak.gov.tr.

Planar waveguide with left-handed material guiding film for refractometry applications

Taher M. EL-AGEZ, Sofyan A. TAYA,* Mohamed M. SHABAT,
Hani M. KULLAB

Physics Department, Islamic University of Gaza, Gaza, Palestinian Authority

Received: 13.06.2012 • Accepted: 02.10.2012 • Published Online: 19.06.2013 • Printed: 12.07.2013

Abstract: A symmetric 3-layer slab waveguide with a left-handed material as a guiding layer is examined analytically for cover refractive index detection. The TM mode dispersion relation of the proposed waveguide is investigated. The sensitivity of the proposed sensor to changes in the cover refractive index and the power flowing within each layer are presented. Some unusual features are found; for example, the sensitivity of the proposed sensor is negative. Moreover, the sensitivity improvement compared with the conventional 3-layer waveguide sensor is approximately a factor of 6.

Key words: Slab waveguides, optical sensors, left-handed material, sensitivity, power

1. Introduction

In 1968, Veselago predicted that substances with negative electric permittivity ϵ and negative permeability μ have some properties different from those with positive values [1]. These materials are usually termed left-handed materials (LHMs) or metamaterials. LHMs are artificially materials having many interesting properties such as negative ϵ and μ and hence a negative refractive index (n). According to Maxwell's curl equations, materials with $\epsilon > 0$ and $\mu > 0$ have electric field \mathbf{E} , magnetic field \mathbf{H} , propagation vector \mathbf{k} , and the direction of energy flux, which is determined by the Poynting vector $\mathbf{S} = \mathbf{E} \times \mathbf{H}$, form a right-handed set of vectors. However, if $\epsilon < 0$ and $\mu < 0$ then they form a left-handed set and the direction of propagation is in the opposite direction of energy flow. The first experimental investigation of negative index of refraction was performed by Shelby et al. in 2001 [2]. Since then, LHMs have been a hot research issue [3–9] in order to design novel types of devices with unconventional properties. Pendry et al. [10] reported one of the first applications of LHMs by demonstrating that a slab of lossless LHM can provide a perfect image of a point source. Grbic et al. [11] verified by simulation the enhancement of evanescent waves in a transmission-line network by using a negative refractive index material. In 2003, it was shown that LHMs can enhance the evanescent field in planar slab waveguides [12]. Recently, LHMs have been proposed as a mechanism of building cloaking devices [13]. Taya et al. proposed an optical slab waveguide sensor using a LHM layer [7].

Optical waveguide sensors can be used to provide information about the presence or concentration of biological molecules or chemical traces in an analyte [14]. Many advantages have been reported for waveguide sensors such as immunity to electromagnetic interference and resistance to harsh environments. These devices are called evanescent field sensors because of their principle of operation. In such devices, the analyte is localized

*Correspondence: staya@iugaza.edu.ps

in the cladding or substrate layer and is probed by the evanescent field of the resonance modes [15–17]. Many efforts have been made to enhance the sensitivity of evanescent field sensors. Very recently, Skivesen et al. proposed the so-called reverse-symmetry waveguide optical sensor [18–20]. In these structures the substrate has a refractive index less than that of the aqueous cladding medium. This design allows deeply penetrating evanescent optical fields into the analyzed cover sample. Metal-clad waveguides for sensor applications have been studied intensively to achieve high sensitivity for refractive index measurements [21]. It was shown that it is possible for metal-clad waveguides to achieve a considerable sensitivity improvement compared to surface plasmon resonance sensors. Taya et al. have introduced Kerr-type nonlinear materials in optical waveguide sensors [22–25]. They presented planar structures in which at least one of the surrounding media has an intensity-dependent refractive index. In these structures, a considerable sensitivity improvement was found due to the optical nonlinearity. Moreover, the sensitivity of waveguide-based sensors was shown to be dramatically enhanced by using an additional layer of LHM between the guiding layer and the cladding [7].

In the present work, a 3-layer waveguide structure with a LHM core layer is investigated for sensing applications. TM waves are considered. The variation in the sensitivity with the parameters of the LHM core layer is presented to find out the optimal structure corresponding to maximum sensitivity. The power flowing within each layer and the power confinements are also investigated.

2. Structure analysis

Figure 1 shows a schematic of the proposed sensor configuration. We consider a slab waveguide with a LHM thin film of thickness d occupying the region $0 < z < d$, and it is characterized by an electric permittivity ε_2 and magnetic permeability μ_2 . The film is sandwiched between 2 semi-infinite media occupying the regions $z < 0$ and $z > d$ and having the parameters (ε_1, μ_1) and (ε_3, μ_3) , respectively. The LHM has been shown to yield an effective electric permittivity and magnetic permeability of the forms [26]

$$\varepsilon_2(\omega) = 1 - \frac{\omega_p^2}{\omega^2 + i\gamma\omega}, \quad (1)$$

$$\mu_2(\omega) = 1 - \frac{F\omega^2}{\omega^2 - \omega_o^2 + i\gamma\omega}, \quad (2)$$

where ω_p is the plasma frequency, ω_o is the resonance frequency, γ is the electron scattering rate, and F is the fractional area of the unit cell occupied by the split ring.

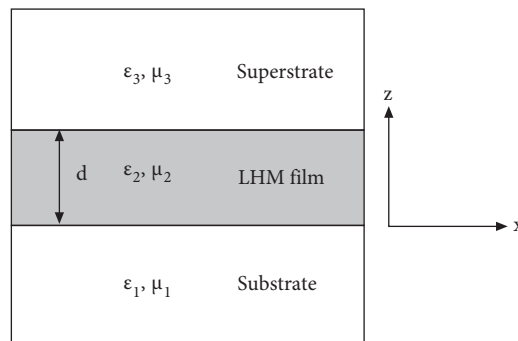


Figure 1. Schematic structure of the proposed sensor.

In order to obtain the dispersion relation, it is necessary to solve Maxwell's equations for the 3-layer structure. The solutions for the time harmonic magnetic fields are given by

$$\vec{H} = \begin{cases} A e^{\beta_1 z} e^{i k_x x} \hat{y} & \text{Substrate region} \\ (B e^{-\beta_2 z} + C e^{\beta_2 z}) e^{i k_x x} \hat{y} & \text{Film region} \\ D e^{-\beta_3(z-d)} e^{i k_x x} \hat{y} & \text{Superstrate region} \end{cases} \quad (3)$$

Using Maxwell's equations we can find the nonvanishing components of the electric field

$$\vec{E} = \begin{cases} -i \frac{\beta_1 A}{\omega \varepsilon_0 \varepsilon_1} e^{\beta_1 z} e^{i k_x x} \hat{x} & \text{Substrate region} \\ i \frac{\beta_2}{\omega \varepsilon_0 \varepsilon_2} (-B e^{-\beta_2 z} + C e^{\beta_2 z}) e^{i k_x x} \hat{x} & \text{Film region} \\ -i \frac{\beta_3 D}{\omega \varepsilon_0 \varepsilon_3} e^{-\beta_3(z-d)} e^{i k_x x} \hat{x} & \text{Superstrate region} \end{cases} \quad (4)$$

$$\vec{E} = \begin{cases} \frac{k_x A}{\omega \varepsilon_0 \varepsilon_1} e^{\beta_1 z} e^{i k_x x} \hat{z} & \text{Substrate region} \\ \frac{k_x}{\omega \varepsilon_0 \varepsilon_2} (B e^{-\beta_2 z} + C e^{\beta_2 z}) e^{i k_x x} \hat{z} & \text{Film region} \\ \frac{k_x D}{\omega \varepsilon_0 \varepsilon_3} e^{-\beta_3(z-d)} e^{i k_x x} \hat{z} & \text{Superstrate region} \end{cases} \quad (5)$$

where $\beta_j = -i k_{z,j} = (k_x^2 - \varepsilon_j \mu_j k_0^2)^{1/2}$; $j = 1, 2$, and 3 ; $k_x = k_0 N$; $k_0 = \frac{2\pi}{\lambda}$; λ is the vacuum wavelength of the guided light; and N is the effective refractive index.

The constants A , B , C , and D , and the longitudinal propagation constants k_x can be determined by applying the boundary conditions, which require that the components of \vec{E} and \vec{H} parallel to the interfaces are continuous. Applying the continuity requirements at $z = 0$ and $z = d$ and with some manipulation, we obtain the dispersion relation for bulk polariton of the TM mode as

$$\left(\frac{k_{z,2}}{\varepsilon_2}\right)^2 - \cot(k_{z,2}d) \left(\frac{\beta_1}{\varepsilon_1} + \frac{\beta_3}{\varepsilon_3}\right) \left(\frac{k_{z,2}}{\varepsilon_2}\right) - \left(\frac{\beta_1 \beta_3}{\varepsilon_1 \varepsilon_3}\right) \mp m\pi = 0. \quad (6)$$

The working principle of this waveguide sensor is to measure the change in effective refractive index due to any change in the cover refractive index medium. Therefore, it is necessary to calculate the sensitivity of the sensors as the derivative of the effective refractive index with respect to the cover refractive index ($n_3 = \sqrt{\varepsilon_3}$). Thus, the sensitivity is usually given by

$$S = \frac{\partial N}{\partial n_3}, \quad (7)$$

where N is the effective refractive index of the guided mode.

Differentiating Eq. (6) with respect to N , the sensitivity of the proposed sensor is found to be

$$S = \frac{G_1}{a_c} \frac{n_3}{N X_c} \left(1 + 2 \frac{a_n X_c^2}{n_3^2}\right) \left(k_0 d + G_1 \frac{q_c}{a_c} + G_2 \frac{q_s}{a_s}\right)^{-1}, \quad (8)$$

where $a_s = \frac{\varepsilon_1}{\varepsilon_2}$, $a_c = \frac{\varepsilon_3}{\varepsilon_2}$, $a_n = \frac{1}{n_2^2 - N^2}$, $X_s = \frac{\beta_1}{k_{z,2}}$, $X_c = \frac{\beta_3}{k_{z,2}}$, $G_1 = \frac{1}{1 + \left(\frac{X_c}{a_c}\right)^2}$, $G_2 = \frac{1}{1 + \left(\frac{X_s}{a_s}\right)^2}$,
 $q_s = \frac{1 + X_s^2}{X_s}$, and $q_c = \frac{1 + X_c^2}{X_c}$.

To study the power propagating in the structure, we calculate the time-averaged Poynting vector $S_x = Re[(\vec{E} \times \vec{H}) \cdot \hat{a}_x]$, The total energy flux can be calculated as $\int_{-\infty}^{\infty} S_x dz$, from which we obtain

$$P_1 = \frac{k_x |A|^2}{4\omega\varepsilon_0 n_1^2 \beta_1}, \tag{9}$$

$$P_2 = \frac{k_x \mu_2}{2\omega\varepsilon_0 n_2^2} \left\{ -i \frac{|B|^2}{2k_{z,2}} (e^{2ik_{z,2}d} - 1) + i \frac{|C|^2}{2k_{z,2}} (e^{-2ik_{z,2}d} - 1) + 2BCd \right\}, \tag{10}$$

$$P_3 = \frac{k_x |D|^2}{4\omega\varepsilon_0 n_3^2 \beta_3}, \tag{11}$$

where the amplitudes are related to each through the relations

$$B = \frac{A}{2} \left(1 - i \frac{\varepsilon_2}{\varepsilon_1} \frac{\beta_1}{k_{z,2}} \right), \tag{12}$$

$$C = \frac{A}{2} \left(1 + i \frac{\varepsilon_2}{\varepsilon_1} \frac{\beta_1}{k_{z,2}} \right), \tag{13}$$

$$D = A \left(1 - i \frac{\varepsilon_2}{\varepsilon_1} \frac{\beta_1}{k_{z,2}} \right) \left(\frac{\varepsilon_3 k_{z,2}}{\varepsilon_3 k_{z,2} + i\beta_3 \varepsilon_2} \right) e^{ik_{z,2}d}. \tag{14}$$

It is instructive to study the percentage of time-average power contained in each region. To quantify the fractional power within the j th layer, we define the confinement factor Γ_j as

$$\Gamma_j = \frac{\text{Time - average power transported in the } j\text{th region}}{\text{Total time - average power transported by the waveguide}}. \tag{15}$$

The following relation must hold between the confinement factors

$$\sum_{j=1}^3 \Gamma_j = 1. \tag{16}$$

3. Numerical results and discussion

In our analysis we consider a symmetric slab waveguide working at the wavelength of a Nd:YAG laser ($\lambda = 1064$ nm) with the surrounding medium being water with $n_1 = n_3 = 1.33$ ($\varepsilon_1 = \varepsilon_3 = 1.77$) and $\mu_1 = \mu_3 = 1$.

The real and imaginary parts of the sensitivity of the proposed sensor as a function of thickness of the LHM film are plotted in Figures 2 and 3, respectively, for different values of γ . The 2 figures show a negative sensitivity, which means that the dependence of the effective refractive index on the cladding index has a negative gradient. This means that the effective refractive index decreases with increasing cladding index. The

real part of the effective refractive index is much more sensitive to variations in the cladding index than is the imaginary part. For a given thickness of the guiding LHM layer and γ , say 150 nm thickness and $\gamma = 0.010\omega_p$, we find from the figures that $\text{Re}(S) = -1.4833$ whereas $\text{Im}(S) = -0.0554$, which means that $\text{Re}(S)$ is 26.77 times larger than $\text{Im}(S)$. This is simply because the cladding index is real and therefore any change in it has a greater impact on the real part of the effective refractive index. As seen in Figure 3, the sensitivity of the imaginary part of the effective index can be slightly improved with increasing γ , whereas $\text{Re}(S)$ is barely affected due to its high value with changing γ in the considered range of γ . In general, both the real and imaginary parts of S show the same behavior with the thickness of the guiding LHM layer. The absolute values of both parts of the sensitivity maximize for low values of d and decay with increasing thickness. In principle, the sensing operation is performed by the evanescent optical field extending from the thin guiding film into the cladding medium. This part of the guided field is generally a few percent and decays with increasing thickness d due to the high confinement of the guided mode. The behavior of both parts of the sensitivity with d is similar to that obtained for the sensitivity of the conventional 3-layer waveguide with a positive index material guiding layer with a reverse symmetry configuration [24,25].

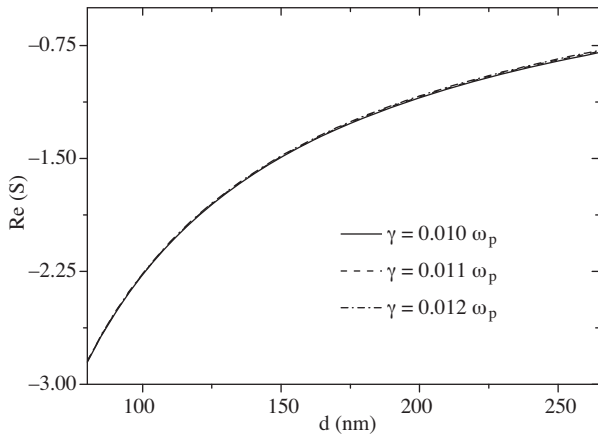


Figure 2. Real part of the sensitivity of the proposed sensor versus the thickness of the guiding LHM layer for different values of the electron scattering rate for $\lambda = 1064$ nm, $n_s = n_c = 1.33$, $\mu_s = \mu_c = 1$, and $F = 0.58$.

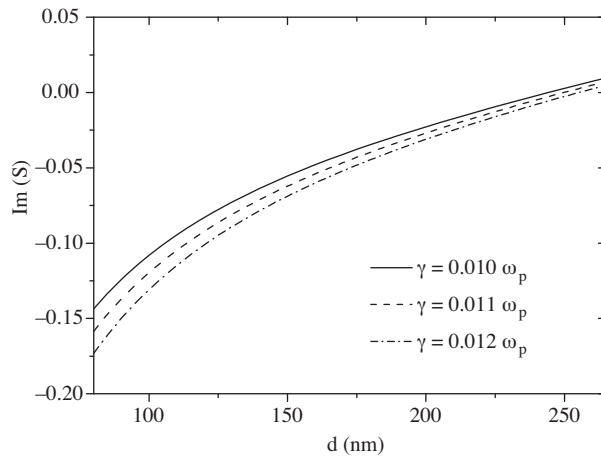


Figure 3. Imaginary part of the sensitivity of the proposed sensor versus the thickness of the guiding LHM layer for different values of the electron scattering rate for $\lambda = 1064$ nm, $n_s = n_c = 1.33$, $\mu_s = \mu_c = 1$, and $F = 0.58$.

It is clear that the proposed sensor has improved sensitivity compared to the conventional ones given in the literature in different forms. To illustrate this point, we assume a symmetric 3-layer waveguide with a lossless positive index material guiding layer. The sensitivity of such a structure is given in the literature [22,25]. In Figure 4, the absolute value of the real part of the sensitivity of the proposed sensor and the sensitivity of the conventional structure are plotted as a function of thickness d . As can be seen from the figure, the sensitivity of the proposed sensor is much higher than that of the conventional 3-layer waveguide sensor. This sensitivity improvement is critically dependent on the thickness of the guiding layer, e.g., for $d = 80$ nm, $d = 100$ nm, and $d = 150$ nm the enhancement is approximately a factor of 5.82, 5.49, and 3.27, respectively. This sensitivity enhancement is attributed to the amplification of evanescent waves caused by LHMs. It was verified that LHMs with low loss can focus light onto an area smaller than a square wavelength in near fields [27]. This super-resolution is also attributed to the important feature of LHMs, which is amplification of evanescent waves [28].

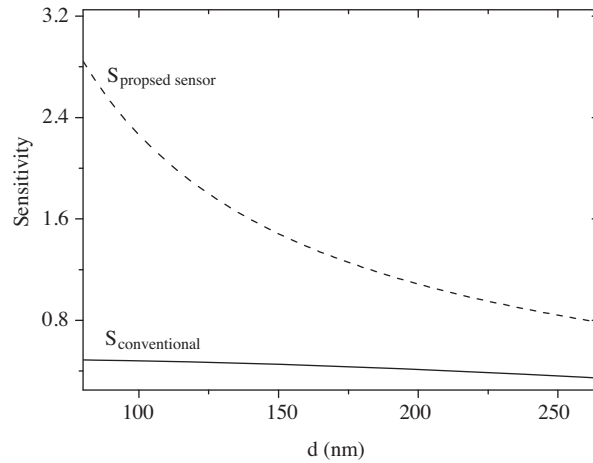


Figure 4. Absolute value of the real part of the sensitivity of the proposed sensor and the sensitivity of the conventional structure as a functions of the thickness of the LHM guiding layer for $\lambda = 1064$ nm, $n_s = n_c = 1.33$, $\mu_s = \mu_c = 1$, $\gamma = 0.012\omega_p$, and $F = 0.58$.

In order to optimize the proposed structure, it is significant to study the sensitivity dependence on different parameters of the LHM guiding layer. We here restrict ourselves to the real part of the sensitivity. As seen by Eqs. (1) and (2), ε_2 and μ_2 are critically dependent on ω , ω_p , and ω_o . Figure 5 shows the real part of the sensitivity as a function of ω_p/ω for different guiding layer thicknesses. In the figure, the range $1.68 < \omega_p/\omega < 2$ (in GHz) has been considered, in which the real parts of ε_2 and μ_2 are both negative to make sure that the guiding layer is made of a LHM. A number of interesting features can be observed in the figure. There is an optimum value of ω_p/ω at which $\text{Re}(S)$ peaks and this optimum value is dependent on the thickness of the guiding layer. The optimum value of ω_p/ω shifts towards higher values as the thickness of the guiding layer increases. For $d = 100$ nm, the optimum value of ω_p/ω is 1.688 whereas it is 1.698 for $d = 145$ nm. The value of the sensitivity at the peak is critically dependent on the thickness of the guiding LHM layer. In the considered range of ω_p/ω and d , the sensitivity at the peaks ranges between -8 and -16 . The most important feature is that through proper choice of ω_p/ω and d , $\text{Re}(S)$ may reach a value of order -16 , which means the enhancement factor of the sensitivity of the proposed sensor could be of order 32. Figure 6 shows the real part of the sensitivity as a function of the thickness of the LHM guiding layer for different values of the resonance frequency ω_o . A considerable increase in the absolute value of $\text{Re}(S)$ is observed with decreasing ω_o . The impact of ω_o on $\text{Re}(S)$ is much greater than that of γ . It is well known that LHMs are artificial multifunctional materials that gain their properties from their structure rather than inheriting them directly from the materials they are composed of. Thus the LHM parameters (ω_p , ω_o , γ) can be controlled by adjusting the structure size. For example, in a recent study, the resonance frequency band of a rectangular periodic structure was found to be shifted and broadened from low to high frequency by adjustment of the corresponding structure size [29]. Therefore, the LHM parameters (ω_p , ω_o , γ) can be adjusted to attain a considerable sensitivity enhancement.

Figure 7 shows the power confinement factors in the film layer Γ_f , cladding layer Γ_c , and substrate layer Γ_s as functions of the LHM thickness for different values of γ . Due to the symmetric configuration assumed in the calculations, there is no cut-off thickness and therefore the size of the guiding layer can go to zero theoretically. The power distributions are in the expected shape. The power confinement factor within the film region increases as the thickness d increases at the expense of Γ_c and Γ_s . Due to the symmetric configuration

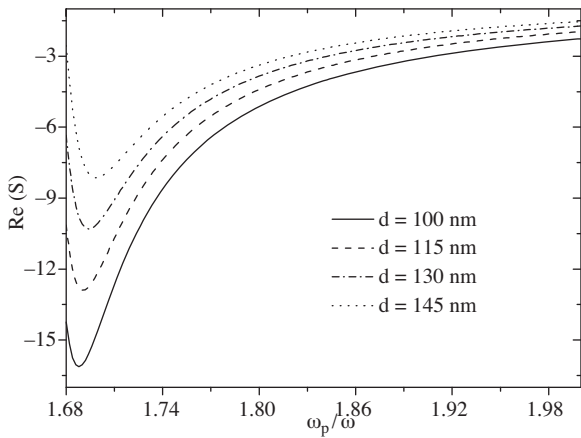


Figure 5. Real part of the sensitivity of as a function of ω_p/ω for different thicknesses of the guiding layer for $\lambda = 1064$ nm, $n_s = n_c = 1.33$, $\mu_s = \mu_c = 1$, $\gamma = 0.012\omega_p$, and $F = 0.58$.

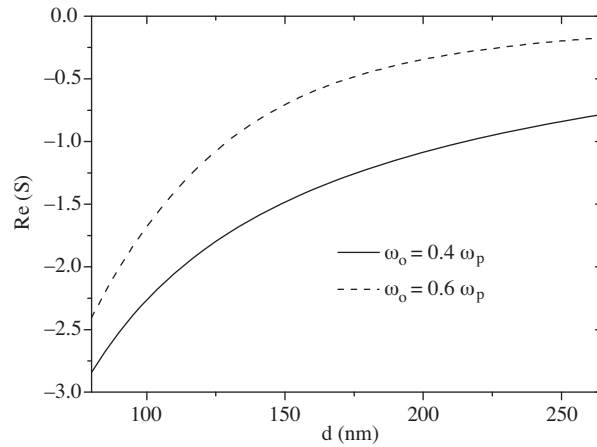


Figure 6. Real part of the sensitivity as a function of d and ω_o for $\lambda = 1064$ nm, $n_s = n_c = 1.33$, $\mu_s = \mu_c = 1$, $\gamma = 0.012\omega_p$, and $F = 0.58$.

assumed Γ_c and Γ_s are identical. The impact of γ on Γ_j is not very big. Increasing γ between $0.010\omega_p$ and $0.012\omega_p$ causes a little enhancement in Γ_c and Γ_s . A well-known feature appears in Figure 7, which is the negative value of Γ_f . This is one of the main differences between negative index and positive index materials. In positive index materials, the Poynting vector \mathbf{S} always forms a right-handed set with the vectors \mathbf{E} and \mathbf{H} . Accordingly, \mathbf{S} and the propagation vector \mathbf{k} are in the same direction. However, this is not the case in LHMs in which \mathbf{S} and \mathbf{k} are in opposite directions. It is well known that the phase velocity and the propagation vector \mathbf{k} are in the same direction for normal materials. Thus, it is clear that LHMs are substances with a so-called negative group velocity, which occurs in particular in anisotropic substances or when there is spatial dispersion [1].

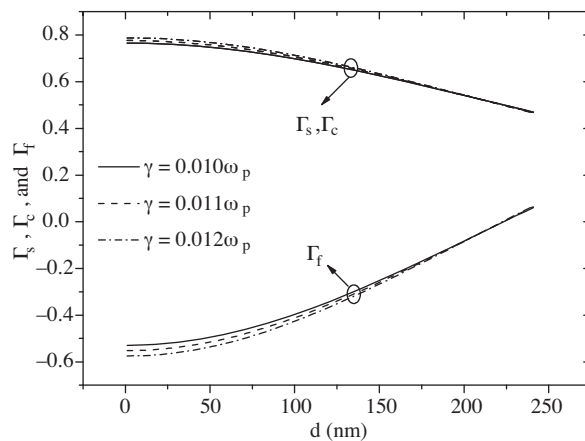


Figure 7. Real part of confinement factors as a function of d and γ for $\lambda = 1064$ nm, $n_s = n_c = 1.33$, $\mu_s = \mu_c = 1$ and $F = 0.58$.

It should be pointed out that the potential fabrication of the proposed LHM film is the frequently used method to realize the negative index of refraction, which combines composite split-ring resonators (SRRs) and

metal wires. The SRRs are used to generate negative permeability whereas the metal wires are used to produce negative permittivity.

Finally, the novelty of this work with respect to one published previously [7] should be stressed. In Taya et al. [7], it was shown that the sensitivity of optical waveguide sensors can be doubled by adding a thin LHM layer between the guiding and cladding layers. In the present work, it was shown that when the guiding layer is made of LHM the sensitivity can be enhanced by any factor depending on the parameters of the LHM. Moreover, the dispersion and imaginary part of ε and μ of the LHM were neglected by Taya et al. whereas they were considered in our work.

4. Conclusion

In this work, we analyzed a 3-layer slab waveguide optical sensor consisting of a LHM core layer. It was shown that the sensitivity of the proposed structure can be enhanced by any factor depending on the chosen parameters of the LHM guiding layer. It is well known that LHMs gain their properties from their structure rather than acquiring them from the materials they are composed of. Thus the LHM parameters can be controlled by adjustment of the structure size to provide novel tools to significantly enhance the sensitivity and resolution of sensors. We think that our results will be helpful for many potential applications in optical evanescent waveguide sensors.

References

- [1] V. G. Veselago, *Sov. Phys. Usp.*, **10**, (1968), 509.
- [2] R. Shelby, D. Smith and S. Schultz, *Science*, **292**, (2001), 77.
- [3] D. R. Smith and N. Kroll, *Phys. Rev. Lett.*, **85**, (2000), 2933.
- [4] R. Ruppin, *Phys. Lett. A*, **227**, (2000), 1811.
- [5] S. A. Taya, T. M. El-Agez, H. M. Kullab, M. M. Abadla and M. M. Shabat, *Optica Applicata*, **42**, (2012), 193.
- [6] M. Abadla, S. A. Taya and M. M. Shabat, *Sensor Lett.*, **9**, (2011), 1823.
- [7] S. A. Taya, M. M. Shabat and H. Khalil, *Optik*, **120**, (2009), 504.
- [8] H. M. Kullab, S. A. Taya and T. M. El-Agez, *J. Opt. Soc. Am. B*, **29**, (2012), 959.
- [9] K. Park, B. J. Lee, C. Fu and Z. M. Zhang, *J. Opt. Soc. Am. B*, **22**, (2005), 1016.
- [10] J. B. Pendry, *Phys. Rev. Lett.*, **85**, (2000), 3966.
- [11] G. Eleftheriades, *App. Phys. Lett.*, **82**, (2003), 1815.
- [12] D. K. Qing and G. Chen, *Appl. Phys. Lett.*, **21**, (2003), 669.
- [13] Alu and N. Engheta, *Phys. Rev. E*, **72**, (2005), 016623.
- [14] D. Kumar and V. Singh, *Optik*, **122**, (2011), 1872.
- [15] O. Parriaux and P. Dierauer, *Opt. Lett.*, **19**, (1994), 508.
- [16] S. A. Taya and T. El-Agez, *Turk. J. Phys.*, **35**, (2011), 31.
- [17] T. El-Agez and S. A. Taya, *Optica Applicata*, **41**, (2011), 89.
- [18] N. Skivesen, R. Horvath and H. Pedersen, *Opt. Lett.*, **28**, (2003), 2473.
- [19] R. Horvath, H. Pedersen, N. Skivesen, C. Svanberg and N. Larsen, *J. Micromech. Microeng.*, **15**, (2005), 1260.
- [20] S. A. Taya and T. M. El-Agez, *J. Opt.*, **13**, (2011), 075701.

- [21] N. Skivesen, R Horvath and H. Pedersen, *Sens. Actuators B*, **106**, (2005), 668.
- [22] S. A. Taya, M. Shabat, H. Khalil and D. Jäger, *Sens. Actuators A*, **147**, (2008), 137.
- [23] S. A. Taya, M. Shabat and H. Khalil, *Optik*, **121**, (2010), 860.
- [24] M. M. Shabat, H. M. Khalil, S. A. Taya and M. M. Abadla, *Int. J. Optomechatronics*, **1**, (2007), 284.
- [25] H. M. Khalil, M. M. Shabat, S. A. Taya and M. M. Abadla, *Int. J. Modern Phys. B*, **21**, (2007), 5075.
- [26] R. Ruppin, *J. Phys.: Condens. Matter*, **13**, (2001), 1811.
- [27] V. A. Podolskiy and E. E. Narimanov, *Opt. Lett.*, **30**, (2005), 75.
- [28] C. Yan, Q. Wang and Y. Cui, *Optik*, **121**, (2010), 63.
- [29] C. Zhang, Z. Yuan, M. Sun, J. Wu and P. Gao, *Appl. Opt.*, **49**, (2010), 281.